Persistent current in an artificial quantum-dot molecule

R. Kotlyar and S. Das Sarma
Department of Physics, University of Maryland, College Park, Maryland 20742-4111
(Received 9 January 1997)

Using an exact diagonalization technique within a generalized Mott-Hubbard Hamiltonian, we predict the existence of a ground-state persistent current in coherent two-dimensional semiconductor quantum-dot arrays pierced by an external magnetic flux. The calculated persistent current, which arises from the nontrivial dependence of the ground-state energy on the external flux, exists in isolated arrays without any periodic boundary condition. The sensitivity of the calculated persistent current to interaction and disorder is shown to reflect the intricacies of various Anderson-Mott-Hubbard quantum phase transitions in two-dimensional systems. [S0163-1829(97)50816-2]

Significant recent advances in semiconductor materials growth and nanolithography techniques now allow[1] for the fabrication of multiple quantum-dot systems in modulation-doped two-dimensional electron structures that are quantum mechanically coherent, and may therefore be considered two-dimensional ''artificial molecules'' (with individual quantum dots being the ''atomic'' constituents of this artificial molecule). Theoretical work on multidot systems has mostly concentrated on the two limiting situations[2,3] (coherent dots with no Coulomb interaction[2] and Coulomb blockade of individual dots[3]). In this paper, we consider coherent two-dimensional (2D) arrays of quantum dots (i.e., 2D artificial molecules) taking into account[4,5] both quantum fluctuations arising from interdot hopping and electron-electron interaction effects through a generalized Mott-Hubbard Hamiltonian.[4] Our main result is the prediction of an *equilibrium persistent current* in finite 2D arrays of semiconductor quantum dots in the presence of an applied magnetic field transverse to the 2D plane. A measurement of this persistent current in small 2D arrays will be definitive evidence for the formation of an artificial quantum-dot molecule. The predicted persistent current is a periodic function of the external flux and exhibits clear signature of the competition between coherence and interaction in artificial 2D molecules. We include disorder effects in our calculation and show that our predicted equilibrium persistent current should be experimentally observable in currently (or soon-to-be) accessible 2D quantum-dot arrays.

It is well known[6–8] that gauge invariance and single valuedness of electron wave functions allow for the existence of a ground-state persistent current in normal metal rings surrounding an external magnetic flux. The intrinsic magnetic moment associated with this persistent current, which is proportional to the current in one-dimensional (1D) rings, is an oscillatory function of the external flux with a period equal to the elementary flux quantum $\phi_0 = h/e$. The existence of such an oscillatory persistent current in normal metal rings has been experimentally verified.[9–11] Our predicted ground-state persistent current in 2D quantum-dot arrays has some significant differences with the existing persistent current theoretical analyses in the 1D ring geometry. The system we consider is a finite coherent 2D quantum-dot array, where the one electron states are in the atomic tight-binding limit (i.e., the electron states tend to be strongly localized on individual quantum dots except for weak interdot quantum tunneling) in contrast to metallic systems that are nearly free-electron-like. In addition, we consider a finite 2D array without any periodic boundary condition in contrast to the 1D ring geometry, which, by definition, is periodic. Another significant aspect of our prediction is the inclusion of quantum tunneling, disorder, and Coulomb interaction effects on equal footings because in real semiconductor quantum-dot arrays all of these effects are expected to be important.

We model the finite square 2D quantum-dot array of size $L_x \times L_y = L$ dots through the following physically motivated generalized 2D Mott-Hubbard type strongly correlated Hamiltonian[4] ($c, c^\dagger$ are electron field operators and $\hat{n}$ is the density operator)

$$H = \sum_{i,\alpha} \varepsilon_\alpha c_{i\alpha}^\dagger c_{i\alpha} + \frac{U}{2} \sum_i \hat{n}_i{}^2 + \sum_{ij} \frac{V_{ij}}{2} \hat{n}_i \hat{n}_j - \sum_{\langle i,j \rangle, \alpha} (t_{\alpha,ij} e^{i\phi_{ij}} c_{i\alpha}^\dagger c_{j\alpha} + \text{H.c.}), \quad (1)$$

where $\phi_{ij} = e/\hbar \int_{ij} \vec{A} \cdot \vec{l_{ij}}$ is the usual Peierls gauge phase factor arising from electron hopping on a lattice in a transverse external magnetic flux (with $\vec{A}$ the vector potential and $\vec{l_{ij}}$ the spatial vector along a plaquette). The indices i, j are the quantum-dot spatial positions in the array and α denotes an electron state on the quantum dot. The generalized Mott-Hubbard parameters U, V, and t have the usual significance of the on-site Coulomb interaction, the long range part of the Coulomb interaction, and the hopping kinetic energy term, respectively, within the tight binding description of the 2D array. We consider two spin-split energy levels ε_α per dot due to quantum confinement in a dot. We assume the magnetic field to be weak enough for single-particle level crossing effects not to be important. We concentrate here on the collective physics in the array in the strongly interacting and noninteracting system limiting cases leaving out the crossover between these two regimes due to single-dot Zeeman physics. The Coulomb interaction in the array is expressed in terms of the capacitance matrix representation.[3] The quantum-dot array is in the tight-binding atomic limit, and

we therefore keep only the nearest-neighbor tunneling term in $t_{ij} \equiv t$. Within the model defined by Eq. (1), U,V,t are parameters to be given as inputs using a physical description of the quantum-dot array.

We are interested in calculating the equilibrium persistent current flowing in the array at $T=0$ in the presence of an external flux threading the 2D lattice. It is easy to show by using commutation properties of H with the polarization operator that the transverse component of the magnetic moment density operator m_z is given by the gauge invariant result

$$m_z = -\frac{\partial H}{\partial \Phi}, \tag{2}$$

where Φ is the total uniform magnetic flux piercing the finite 2D system. (We note that the external magnetic field is in the z direction and with the 2D array in the x-y plane, and therefore m_z is the only nonzero component of the magnetization density.) A nonzero value of the static magnetization density, as measured by a finite m_z, is equivalent to the existence of a ground-state persistent current (whose strength is exactly the same as the measured value of m_z because of the two-dimensional nature of the problem). Our goal is to calculate the equilibrium magnetic moment density for 2D quantum-dot arrays using Eqs. (1) and (2). An experimental measurement of a finite m_z (as a function of external flux) will be a direct verification of the quantum-dot molecule formation.

To obtain the equilibrium persistent current $I \equiv m_z$, we calculate the ground-state energy by doing an *exact diagonalization* of H, defined by Eq. (1), in the basis of the total number of electrons N in the array and the total spin S_z in the direction of the field, and then perform minimization over S_z to find the stable ground state. The magnetic moment density in a finite 2D quantum-dot array is calculated using Eq. (2). Existing semiconductor nanofabrication techniques are *at best* capable of producing coherent arrays that are 2×2 to 3×3 quantum dots in size. The Lanczos diagonalization technique that we use is capable of giving the exact interacting ground state for up to a 3×3 array of our interest. We calculate the persistent current in *interacting* 2D arrays up to $L=3\times3$ sizes for all band fillings n $(=N/2L)$ by varying the number of electrons N in each system between $N=1$ and $N=L$. We use realistic Mott-Hubbard parameters that approximately correspond to 2D GaAs quantum-dot systems (at $T=0$). We choose[4] the intradot single-particle level spacing $\Delta=0.3$ meV to be comparable in magnitude to the interdot hopping parameter $t=0.1$ meV, with the intradot Coulomb charging energy $U\sim1$ meV. With this choice of parameters the 2D quantum-dot array is in the interesting coherent ''molecular'' state referred to as the ''collective Coulomb blockade'' regime,[4] where both coherence and interaction play comparable nonperturbative roles, and the Coulomb blockade of individual dots is destroyed. Disorder is included in our calculation through a spin-independent parameter $W\sim\Delta$ that denotes the half-width of a uniform distribution of random on-site quantum-dot energies centered around Δ. The spin splitting (set to be 0.03Δ that allows us to study the total spin transitions due to the collective motion in the array) of the single-particle energy levels is assumed to be independent of W.

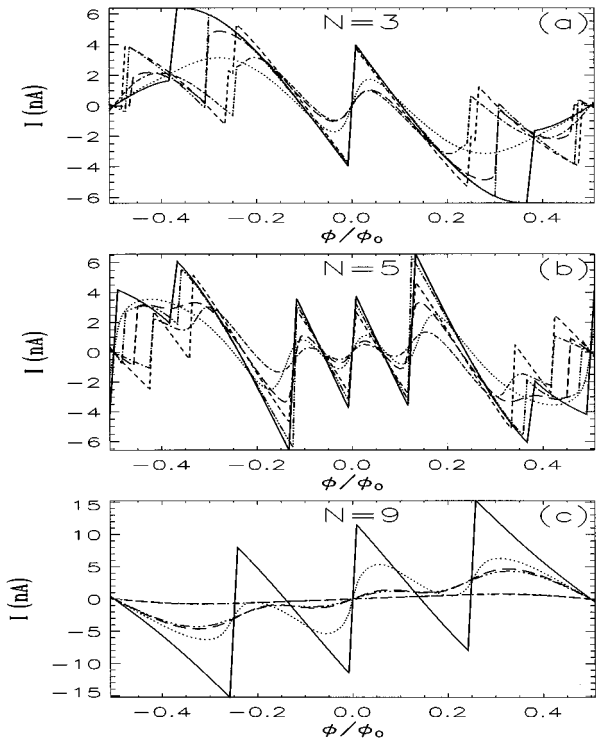

FIG. 1. Typical calculated persistent current for three different values of band filling $[n=1/6(a),5/18(b),1/2(c)]$ in the 3×3 array is plotted versus the magnetic flux through the elementary cell in units of ϕ_0 for six different sets of U,V,W (see the legend in the Fig. 2 for the key to each line in the plot) in the 3×3 system.

We show our typical calculated persistent current as a function of the external flux in Fig. 1 for three different values of band filling $(n=1/6,5/18,1/2)$ in the 3×3 system. Results for six different situations (as described in the figure captions) for various values U, V, and W are shown for each filling with t; Δ is fixed throughout the calculation. The flux ϕ is through each elementary cell (or plaquette) of the 3×3 system, and the calculated equilibrium persistent current is in absolute units. The most significant feature of Fig. 1 is the existence of a persistent current, which is periodic in ϕ/ϕ_0 (*note* that the total flux through the system is $\Phi=4\phi$ by virtue of the four equivalent plaquettes in the 3×3 quantum-dot array), whose magnitude is reasonably large $(\geqslant nA)$. The magnitude of the current depends, in a rather complicated way, on the Mott-Hubbard parameters U, V, and W, and also on the band filling (in particular, on whether $n=1/2$ or not). We can, however, make the following qualitative observations:

(1) Away from half filling, finite disorder is the most prominent destructive effect on the current amplitude, with finite interaction $(U,V\neq0)$ producing some enhancement of the disordered current but never to the free electron $(U,V,W=0)$ value. Without any disorder $(W=0)$, finite U and V have reasonably small effects on the current magnitude away from half filling.

(2) At half filling, however, finite on-site Coulomb repulsion $(U\neq0)$ by itself dramatically suppresses the persistent current with the long-range Coulomb interaction $(V\neq0)$ opposing this dramatic suppression due to finite U.

(3) Disorder, by itself $(W\neq0, U, V=0)$, seems to produce

similar quantitative suppression of the persistent current at all fillings except at half filling, where disorder enhances (slightly) the interacting clean system current.

(4) Long-range Coulomb repulsion ($V\neq 0$) always enhances the current magnitude from its finite U and W values.

(5) The various structures (jumps and discontinuities) in the current arise from many-body energy level crossings that occur in the system at specific fillings and values of the magnetic flux. The discontinuities of the persistent current seen in Fig. 1 correspond to the change of the total orbital momentum in the 2D array, which can be accompanied by spin-flip transitions in the system. Finite disorder ($W\neq 0$) smoothens the discontinuities in the noninteracting ($U,V=0$) current, and removes some of the discontinuities in the interacting ($U,V\neq 0$) current. There are no discontinuities or spin flips at half filling in the interacting system [Fig. 1(c)].

(6) The sign of the persistent current at zero magnetic flux is generally dependent on the electron filling and the geometry of the array. We find the interacting ($U\neq 0$, V, $W=0$) persistent current in 2×2, 3×2, 4×2, and 3×3 arrays to be diamagnetic for $n=1/2L$ and paramagnetic for $n=1/2$. The random disorder of strength W ($=\Delta$, as used in our calculations) does not change the sign of the persistent current.

(7) The current distribution in the clean 2D array is determined by the spatial symmetries of the system and band filling in the array. In the clean 3×3 lattice the current flows along the boundary for all electron fillings in the system. However, the persistent current distribution is disorder realization dependent.

The most important feature of our results, the strong suppression of the persistent current at half filling by the on-site Coulomb repulsion U, is a direct *finite size* manifestation of the Mott-Hubbard metal-insulator transition, which is a true phase transition in the thermodynamic limit. The long-range Coulomb repulsion ($V\neq 0$) opposes this transition in a finite system (leading to an enhancement in the finite U-suppressed current amplitude for $V\neq 0$ at half filling). Effects of finite V and W on the Mott-Hubbard transition in a 2D Hubbard model (in the thermodynamic limit) are not rigorously known, but our results are consistent with the expectation that, in general, finite values of V and W should oppose the metal-insulator Mott transition at half filling. To further quantify the relative magnitudes of the effects of finite U,V,W on the persistent current at various band fillings, we show in Fig. 2 our calculated root-mean-square current amplitude as a function of the number of electrons in the 3×3 quantum-dot array for various values of Mott-Hubbard parameters. The rms current magnitude $\langle I^2\rangle^{1/2}$ is obtained by averaging the typical current (Fig. 1) over one flux period. The six different parameter sets with different values of U,V,W in Fig. 2 clearly show the dominant effect of the Mott-Hubbard transition (for finite U) at half filling ($N=9$) and the generic destructive effect of finite disorder at all fillings, as well as the generic tendency of the long-range Coulomb interaction to homogenize the electron density in the system[12] and consequently to enhance the persistent current.

In the well-studied single 1D ring geometry, the effect of disorder (in the absence of any Coulomb interaction) on the persistent current is an exponentially strong suppression[13] of

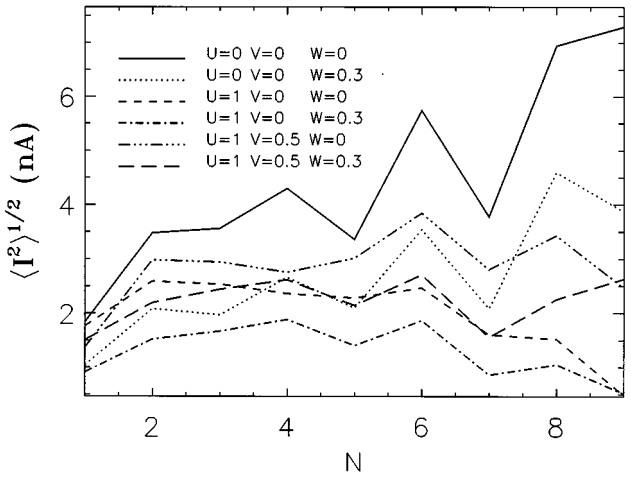

FIG. 2. A plot of the RMS persistent current $\langle I^2\rangle^{1/2}$ versus the number of electrons N in the 3×3 array for the six different sets of U,V,W (as shown in the legends) in the 3×3 system. All energies are given in the meV units.

the current arising from the Anderson localization phenomenon associated with all electronic states being exponentially localized in one dimension in the presence of any finite disorder. For our 2D quantum-dot array the effect of finite disorder ($W\neq 0$) is subtle (and much softer than in one dimension) because localization effects are logarithmically weak[14] in two dimensions for small W. (In fact, in the presence of an external magnetic field breaking the time reversal symmetry, the localization effect is even weaker[14] and may be hard to discern in a finite sample.) This explains the rather benign effect of having a finite W in Figs. 1 and 2 of our results, which should be contrasted with 1D ring calculations where the persistent current is strongly suppressed by finite values of W. To better quantify our finite disorder results we show in Fig. 3 a log-log plot at half filling of the rms current $\langle I^2\rangle^{1/2}$ without any interaction effects ($U,V=0$), averaged over 100 disorder realizations for each value of W, as a function of the disorder strength W for various system sizes (3×3,4×4,5×5,6×6). In plotting these results, we have factored out a scale factor $n_c=(L^{1/2}-1)^2/L$ so that the results for various system sizes fall on top of each other, showing approximate current scaling with system size and disorder. [The scale factor $n_c=(L^{1/2}-1)^2/L$ is the number of unit cells or plaquettes in each square array of size L.] All four noninteracting disordered results scale very well, whereas the one disordered result *with* interaction deviates from the universal scaling at low disorder strength, where the Mott metal-insulator transition effect dominates. The two dashed straight lines in Fig. 3 give the best fits to weak and strong disorder scaled currents, leading to the following empirical results for the effect of disorder on the persistent current: $\langle I^2\rangle^{1/2}=(L/n_c)g(W)$, with the scaling function $g(W)$ being given by

$$g(W)\sim\begin{cases} W^{-\gamma}, & \gamma=(6.4\pm 2.8)\times 10^{-2}, \quad W<1.55\pi t \\ W^{-\beta}, & \beta=1.84\pm 0.49, \quad W>1.55\pi t. \end{cases}$$

The very small value of the scaling exponent γ in the weak disorder limit is consistent with the expected logarithmic weak localization[14] in a 2D array, which eventually crosses

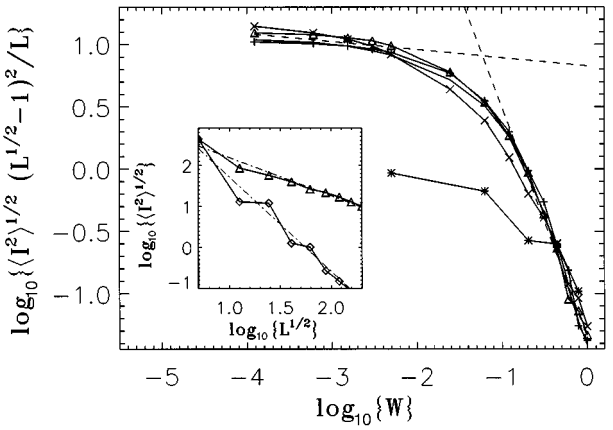

FIG. 3. A log-log plot of $\langle I^2\rangle^{1/2}$ versus W averaged over 100 disorder realizations for each value of W is shown ($U=V=0$) at half filling in 3×3 (crosses), 4×4 (triangles), 5×5 (solid line), 6×6 (pluses). Asterisks show the interacting ($U=1$ meV, $V=0$) results at half filling for the 3×3 system. Inset: $\langle I^2\rangle^{1/2}$ at half filling versus system sizes (L): triangles (2D array), squares (1D ring). (The average is taken over the range of the same total flux through the systems, which varies from $-\phi_0/2$ to $\phi_0/2$.) The dashed lines in the plot are the best linear fits to the corresponding data as described in the text.

over to strong localization for large W. We also expect interaction effects to be particularly important at weak disorder, but not so at high disorder, which is what is seen in Fig. 3 even at half filling. Weak disorder, in fact, produces an antilocalization effect [Figs. 1(c) and 2] at half filling *in the presence of finite U*, by slightly enhancing the persistent current from its finite U-suppressed value. Whether these last two findings remain true in the thermodynamic limit is, however, unknown.

Note that the scale factor n_c in Fig. 3 indicates that the persistent current scales with the perimeter size of the array or the square root of the number of dots $L^{1/2}$ in the system. We have explicitly verified this system size dependence by doing calculations for various system sizes at various fillings. As an example, we show as an inset of Fig. 3 a comparison of the system size dependence of the rms current in the 1D ring and the 2D array geometries, finding an approximately linear dependence on L^{α} with the best fit $\alpha\approx 0.46$ (1.1) in the 2D array (1D ring). Thus, the persistent current is proportional to the length of the boundary in both the 1D ring and the 2D array geometry.

In conclusion, we predict, based on an exact diagonalizaton study of the generalized disordered Mott-Hubbard Hamiltonian, the existence of a ground-state persistent current in finite 2D quantum-dot arrays that should be experimentally observable. Direct observation of an equilibrium persistent current in coherent 2D quantum-dot arrays will not only verify the formation of an artificial quantum-dot molecule but will also shed light on the interplay among coherence, disorder, long- and short-range Coulomb interaction effects on Anderson-Mott-Hubbard quantum phase transitions.

The authors thank Charles Stafford for useful discussions during the early part of this work. This work was supported by the U.S.–O.N.R.

[1] F. R. Waugh *et al.*, Phys. Rev. B **53**, 1413 (1996); R. H. Blick *et al., ibid.* **53**, 7899 (1996); F. Hoffman *et al., ibid.* **51**, 13 872 (1995); N. C. van der Vaart *et al.*, Phys. Rev. Lett. **74**, 4702 (1995); D. Dixon *et al.*, Phys. Rev. B **53**, 12 625 (1996).
[2] G. Kirczenow, Phys. Rev. B **46**, 1439 (1992).
[3] A. A. Middleton and N. S. Wingreen, Phys. Rev. Lett. **71**, 3198 (1993).
[4] C. A. Stafford and S. Das Sarmas, Phys. Rev. Lett. **72**, 3590 (1994).
[5] G. Klimeck, G. Chen, and S. Datta, Phys. Rev. B **50**, 2316 (1994); **50**, 8035 (1994).
[6] F. London, J. Phys. Radium **8**, 347 (1937).
[7] N. Byers and C. N. Yang, Phys. Rev. Lett. **7**, 46 (1961).
[8] M. Buttiker, Y. Imry, and R. Landauer, Phys. Lett. **96A**, 365 (1983).
[9] L. P. Levy *et al.*, Phys. Rev. Lett. **64**, 2074 (1990).
[10] V. Chandrasekhar *et al.*, Phys. Rev. Lett. **67**, 3578 (1991).
[11] D. Mailly *et al.*, Phys. Rev. Lett. **70**, 2020 (1993).
[12] T. Giamarchi and B. S. Shastry, Phys. Rev. B **51**, 10 915 (1995), and references therein.
[13] Ho-Fai Cheung *et al.*, Phys. Rev. B **37**, 6050 (1988).
[14] D. Belitz and T. Kirkpatrick, Rev. Mod. Phys. **66**, 261 (1994).